

# Photonic Integrated Circuits

Thomas L. Koch  
Uziel Koren

A semiconductor laser contains a light-amplifying gain medium and a miniature waveguide that confines the light to the laser cavity. With today's laser-fabrication technology, one can integrate lasers with other active optical elements—such as detectors, optical amplifiers, optical modulators, and switches—on one semiconductor chip. The interconnections are miniature, transparent, passive waveguides that pipe light from one device to the next, playing a role similar to the metal lines that carry electricity in conventional integrated circuits. An exploratory technology to create such photonic integrated circuits is emerging from advances in vapor-phase crystal growth and large-area wafer processing. Initial research efforts are focused on relatively simple devices such as laser-modulator, laser-detector, and laser-amplifier photonic integrated circuits. These configurations enhance the functional capabilities of a single laser, promising advantages in cost, compactness, and ease of packaging. Although today's complex optical systems require large optical benches and many delicate optical alignments, one can also envision these systems transformed into miniature, inexpensive, and robust photonic integrated circuits. Recent research demonstrations of such single-chip circuits include wavelength-division-multiplexing transmission sources and balanced heterodyne receivers.

## Introduction

For many communications engineers, the term *optics* conjures up images of a lens maker's formulas, precision microscopes, and fine camera equipment. However, it was just over two decades ago when S. E. Miller wrote his now-famous article, "Integrated Optics: An Introduction," which was published in the *Bell System Technical Journal*.<sup>1</sup> More than coining a new term, Miller prophesied in his introduction:

*... a miniature form of laser beam circuitry ... Photolithographic techniques may permit simultaneous construction of complex circuit patterns ... possible miniature forms for a laser, modulator, and hybrids. If realized, this new art would facilitate isolating the laser circuit assembly from thermal, mechanical, and acoustic ambient changes through small overall size; economy should ultimately result.*

In the intervening years, the term *integrated optics* has been used most frequently to describe waveguide devices on transparent substrates, such as glass or lithium niobate. On the other hand, lasers for telecommunications are built primarily on III-V semiconductors, usually indium phosphide (InP) substrates. A new term, *photonic integrated circuits* (PICs), has been introduced<sup>2</sup> to describe the semiconductor implementation of Miller's vision. PICs monolithically combine, on a single semiconductor substrate, optically interconnected active elements—such as lasers, modulators, switches, and detectors—with filters, couplers, and other guided-wave components.<sup>3</sup> (Panel 1 defines terms and acronyms.)

PIC technology aims to replace the separate, sequential alignment of single-mode fiber connections between discrete devices

**Panel 1. Abbreviations, Acronyms, and Terms**

CBE — chemical-beam epitaxy  
DBR — distributed Bragg reflector  
DFB — distributed feedback  
 $\epsilon_{LO}$  — optical field amplitude of the local oscillator  
 $\epsilon_{sig}$  — optical field amplitude of the signal  
IC — integrated circuit  
InP — indium phosphide  
InGaAs — indium gallium arsenide  
InGaAsP — indium gallium arsenide phosphide  
 $\Lambda_g$  — period of the corrugation  
 $\lambda_{PL}$  — photoluminescence wavelength  
LO — local oscillator  
MOVPE — metal-organic vapor-phase epitaxy  
MQW — multiple quantum well  
 $n$  — effective index of refraction of the waveguide  
 $n^+$  — heavily doped material in which electrons carry the current  
 $\Omega$  — beat or intermediate frequency  
 $\omega$  — optical frequency of incoming signal  
OEIC — optoelectronic integrated circuits  
 $p^+$  — heavily doped material in which holes carry the current  
 $p$ -type — a material that contains positive dopants  
PIC — photonic integrated circuit  
SEM — scanning electron micrograph  
SI — semi-insulating (doped with iron)  
SI-InP — semi-insulating indium phosphide  
III-V — compound of materials from Groups III and V of the Periodic Table of Elements  
TDM — time-division multiplexing  
WDM — wavelength-division multiplexing

with lithographically produced single-crystal waveguides. (See Panel 2.) This approach not only replaces the costly labor of individual alignments with a wafer-scale batch process, but also produces a lower loss, lower reflection connection and a rugged and reliable package.

During the past few years, substantial progress has been made in this area. In this paper, we discuss the driving forces and technological advances behind this progress. We also highlight the advances with a selection of experimental InP-based PICs built and evaluated recently at AT&T.

**Why PICs Now?**

What warrants such serious interest in optical integration at this time? Transmission rates have already reached into the multi-gigabits-per-second range in today's point-to-point, optical-fiber telecommunications

systems. But as span lengths and speeds continue to increase, it may no longer be acceptable to encode the laser beam by directly modulating the drive current to the laser. The reason is that undesirable dynamic wavelength shifts occur in directly modulated lasers, and these wavelength shifts cause dispersive signal distortions. Instead, we may need some form of modulation or encoding of the laser beam, external to the laser.

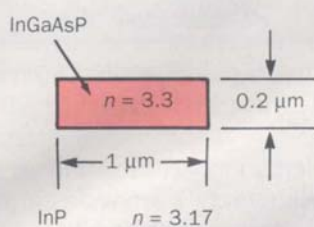
Demands for increased capacity also suggest that wavelength-division-multiplexing (WDM) may be desirable. With WDM, several laser signals may be combined without interference on a single fiber because each signal may be at a different optical wavelength or "color." By combining a set of lower data rate signals, each on a different wavelength channel, we can achieve a high, aggregate transmission rate, yet lessen the demands on the transmitter and receiver electronics that can run at the lower, single-channel rate.

Both external modulation and WDM entail an increased level of optical complexity, with a variety of interconnected optical components at each terminal of the fiber link. Besides components that combine (i.e., multiplex) and separate (i.e., demultiplex) the beam, WDM systems may also require tunable lasers.

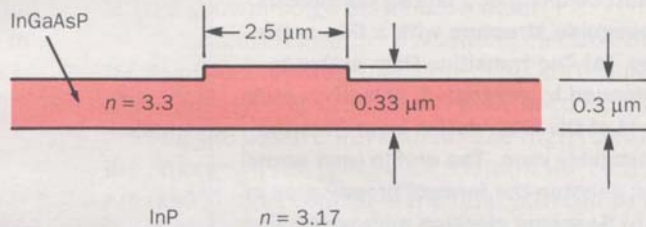
Beyond point-to-point applications, much of the current research is aimed at exploring the role of photonics in a host of new networking and switching architectures. Some of the architectures are based on WDM or even *coherent* techniques, where many principles that are routinely applied in the now-mature radio communications technology can be borrowed directly with a millionfold increase in frequency. Other approaches use ultra-short-pulse laser technology with time-division-multiplexing (TDM). In the TDM approaches, bits for each channel occupy only a short slice of a base time period, and fast optical switches route the bits for each channel to their destinations.

All the approaches share increased optical complexity, compared to today's point-to-point links. Often, the experimental systems consist of a large optical bench filled with interconnected devices.

The hurdle to overcome then, beyond reducing the individual chip cost of each component, is the laborious and costly fiber alignment to each device. In particular, most active, guided-wave, semiconductor devices are optimized with tightly confined optical beams. Such beams require almost impossibly tight focusing and



(a) Buried-heterostructure waveguide



(b) Buried-rib waveguide

### Panel 2. PIC Waveguides

By piping light from one optical device to the next, the tiny waveguides depicted here play a role in PICs that is analogous to the role of metal lines for electrons in electrical integrated circuits. We show cross-sections of two common types of PIC waveguides.

The first (diagram a) is termed a *buried-heterostructure* waveguide. Here, a strip of semiconductor crystal that has a higher index of refraction is surrounded on all sides by a different, but lattice-matched, crystal that has a lower index of refraction. As is true for glass optical fibers, total internal reflection guides the light along such a structure. However, the larger index differences that are encountered between different crystal types permit much smaller, tightly confined waveguides. (Typically, the magnitude of the index difference is about 0.1 or more.) These waveguides have mode sizes of 1  $\mu\text{m}$  and sometimes less, compared to about 6  $\mu\text{m}$  or so for single-mode fibers. Here, typical waveguide dimensions might be 0.2  $\mu\text{m}$  high by 1.0  $\mu\text{m}$  wide, and the waveguide core may contain a complex stack of layers (which have been omitted from the diagram for simplicity). These

buried-heterostructure waveguides are often used for lasers or other devices that are optimized with tightly confined optical energy.

The second type (diagram b) is a *buried-rib* waveguide. Here, the index difference in the lateral dimension is provided by only a small height change (perhaps, a 0.03- $\mu\text{m}$  high rib on a 0.3- $\mu\text{m}$  thick waveguide layer). By using material-selective chemical etches and special ultrathin etch-stop crystal layers (not shown here for simplicity), one can precisely control the rib height. Typical widths for these waveguides might be about 2.5  $\mu\text{m}$ .

Low propagation loss for longer path-length interconnections is easier to achieve on the PIC that has the buried-rib waveguide because of the lower scattering loss from fabrication imperfections. Also, the processing used to form the buried-rib waveguide is more amenable to precise definition of the waveguide geometry. Therefore, these waveguides are ideally suited for couplers and other beam-combining structures, where the geometry is extremely important. Buried-rib waveguides have exhibited only a few percent of waveguide loss per centimeter of propagation distance.

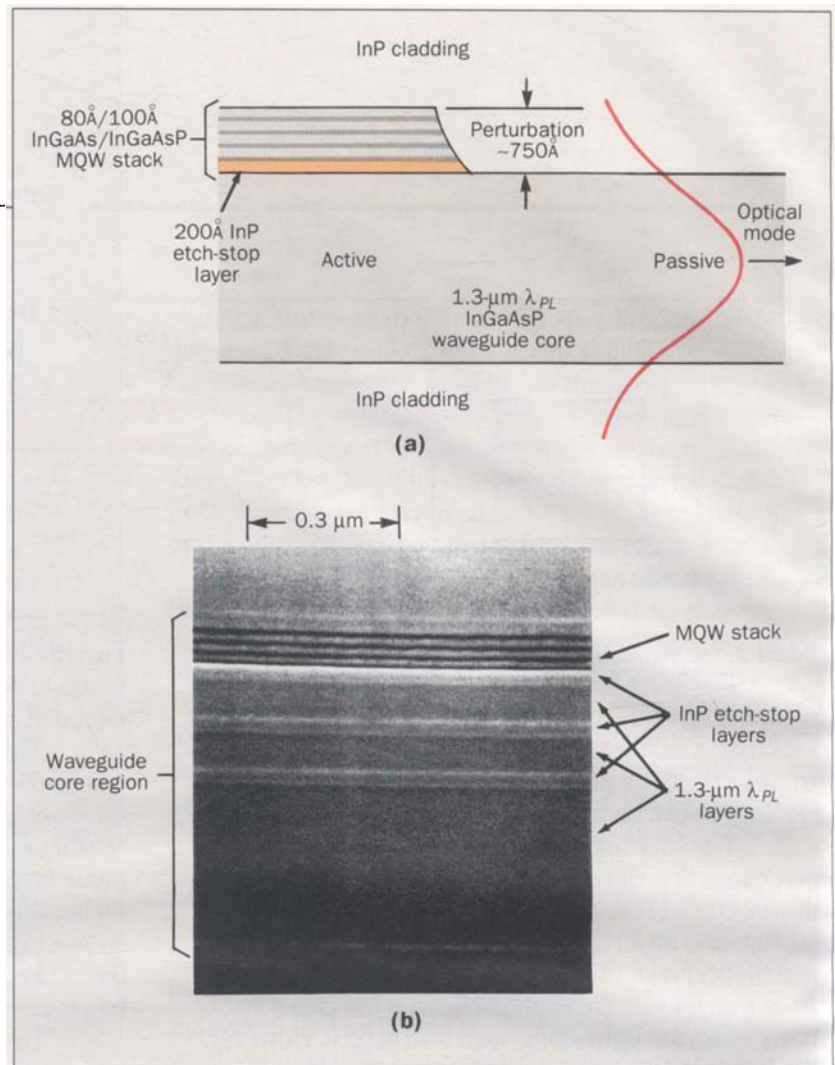
difficult fiber-alignment tolerances.

Even for a single "fiber pig-tailed" laser, a significant and often dominant fraction of the manufacturing cost can reside in the packaging associated with a rugged and efficient fiber connection. (A *fiber pig-tailed laser* is a laser that is inserted in a sealed canister and has an optical fiber, i.e., the pig tail, permanently aligned and attached to provide the laser output.) This cost may be marginally tolerable in today's high-performance links where few such connections are needed. However, it soon becomes unacceptable when we think about and plan for the higher connectivity architectures mentioned

earlier. In extremely cost-sensitive applications such as *fiber to the home* (FTTH),<sup>4</sup> economies realized by integration may be instrumental to successful deployment.

In addition to the probable market pull discussed above, technological advances are also helping to push the PIC technology out of the research lab. Chief among these advances is the availability of high-quality vapor and beam growth techniques for the InGaAsP/InP materials system.<sup>5</sup> (The notation *InGaAsP/InP* means structures that consist of layered, lattice-matched crystals of indium gallium arsenide phosphide and indium phosphide.) This material system is central to the light

**Figure 1. Butt-coupling of a largely continuous, passive waveguide structure with a thin active layer on top. (a) The transition from active to passive is formed by controlled, selective, etch-stop removal of the MQW active layer from the passive waveguide core. The profile (and arrow) on the right denotes the forward propagation of the light. (b) Scanning electron micrograph of a stained cross-section of the waveguide structure. An active stack of four quantum wells (QWs) on top of a 1.3- $\mu\text{m}$   $\lambda_{PL}$  core contains additional InP etch-stop layers for further passive-waveguide processing.**



emitters and detectors used in the 1.3- $\mu\text{m}$  (micrometer) and 1.5- $\mu\text{m}$  wavelength ranges where optical fiber has very low transmission losses. These techniques include metal-organic vapor phase epitaxy (MOVPE) and chemical-beam epitaxy (CBE), which have both yielded highly uniform, large-area epitaxial growth.

These modern growth techniques can easily produce the ultrathin layers (typically, about 20Å to 100Å thick) needed for the quantum wells that are widely used in high-performance optoelectronics devices. Furthermore, the techniques can reproducibly grow highly complex, layered structures, including a multiplicity of the ultrathin etch-stop layers used to permit fabrication of the sophisticated PIC architectures.

Before proceeding, we note that PICs can be considered a subset of a larger field referred to as optoelectronic integrated circuits (OEICs). But in OEIC research, the emphasis has been to integrate the terminal optical transmit or receive device (or arrays of such devices without optical interconnections) with the associated amplification or signal-conditioning electronics.

#### PIC Designs and Examples

The challenge that faces a PIC designer is to combine device requirements that often conflict, yet do it without introducing undue processing or crystal-growth complexity. Problems may stem from the conflicting electrical requirements, perhaps in semiconductor doping or in the level of electrical isolation required between devices. Other problems may stem from the different optical-materials requirements or from the waveguide types needed in the different optical devices. The PIC designer's goal is to maximize common processing steps. Wherever possible, he or she must avoid the philosophy that each completed device stage must be etched away locally to make room for another fabrication sequence for the next optically mated device. Some promising techniques to address these issues will be illustrated in the sections that follow.

**Coupling at Transitions.** Critical to the success of the PIC technology is the ability to make reproducible, high-quality transitions between the active and passive waveguides.

---

In this context, *active* refers to a waveguide that contains material whose bandgap energy is less than or close to the propagating photon energy. Active waveguides are the key parts of the active devices on a PIC. Examples are:

- The gain medium of a laser or amplifier
- The absorbing layer of a waveguide photodetector
- Perhaps, a medium used as an electroabsorption modulator with a suitable applied field.

*Passive* waveguides have a bandgap energy that is substantially greater than the propagating photon energy. These waveguides will exhibit low losses apart from the scattering and residual absorptive losses (such as free-carrier or inter-valence-band absorption) that arise from doping.

To date, most experimental PICs have used some form of butt-coupling. Here, one end of the active waveguide of a particular vertical or lateral structure mates with the passive waveguide of a different vertical or lateral structure. The most straightforward approach uses selective, wet-chemical etching to remove the core stack of the entire active waveguide, and follows this by regrowing a mated, aligned, passive waveguide structure.<sup>6</sup> The principal advantage of such an approach is the independent selection of compositional and dimensional design parameters for the two waveguides. However, this independence comes at some expense; i.e., the increased difficulty of obtaining a reproducible geometry in the crystal regrowth at the joint.

Another approach to butt-coupling uses a largely continuous, passive waveguide structure with a thin active layer on top. The active layer is selectively removed from the portions of the structure that are to be passive. The example in Figure 1a shows a thin, multiple-quantum-well (MQW) active stack, with four quantum wells. An InP etch-stop layer, about 200Å thick, separates the stack from a passive waveguide core. The core is about 0.3 μm thick and is composed of InGaAsP (indium gallium arsenide phosphide) with a photoluminescence wavelength ( $\lambda_{PL}$ ) of 1.3 μm. (It is common to specify thick layers and wavelengths in micrometers and the thickness of thin quantum wells in angstroms. The units differ in magnitude by 10,000.) By using wet-chemical etches that are material selective, we can remove the MQW stack with high reproducibility and precision. Thus, dimensional control is placed in the original, computer-automated

MOVPE growth stage of the base wafer.

Figure 1b shows a scanning electron micrograph (SEM) of such a waveguide core. This core contains additional etch-stop layers that are to be used later for processing the passive waveguide. The high uniformity of the layers and the precise locations of the etch-stop layers permit tight control of the final active-to-passive coupling geometry.

This design also makes use of the high gain achieved in the small net vertical thickness of an MQW gain layer. The removal of the stack, which is about 700Å thick, constitutes only a small perturbation in the bulk of the waveguide core, which consists of the lower, thicker 1.3-μm  $\lambda_{PL}$  layer. With proper design, we can achieve coupling efficiencies of more than 90 percent.

This type of butt-coupling has been used in many of the PICs we describe in the remainder of this paper.

**Gratings for Integration.** Another advance critical to PIC technology is the corrugated-waveguide grating. Fabrication of these gratings became routine after the distributed-feedback (DFB) laser was adopted worldwide as the preferred optical-telecommunications source where high spectral purity is required. These gratings provide high-quality, on-chip resonators without the awkward constraints imposed by the usual cleaved-facet resonators used in semiconductor lasers. In addition, the gratings may also function as filters in some receiver and amplifier applications.

Figure 2, an SEM of the waveguide in a DFB laser, shows the characteristic corrugated interface between a higher index core material and a lower index cladding material. As a light beam propagates down such a waveguide, each bump reflects a small portion of the light. Unless the beam's wavelength is close to the Bragg wavelength, all the reflections are out of phase and interfere destructively. (The *Bragg wavelength* is  $\lambda \approx 2n\Lambda_g$ , where  $\Lambda_g$  is the period of the corrugation and  $n$  is the effective index of refraction of the waveguide.) Near the Bragg wavelength, all reflections add in phase, which leads to a large cumulative reflection.

The corrugations, which have typical periods of about 0.2 μm, are most often fabricated using two ultraviolet laser beams to form an interference pattern on a wafer that is coated with photoresist. When developed, this "holographic" exposure provides a mask for etching the corrugation.

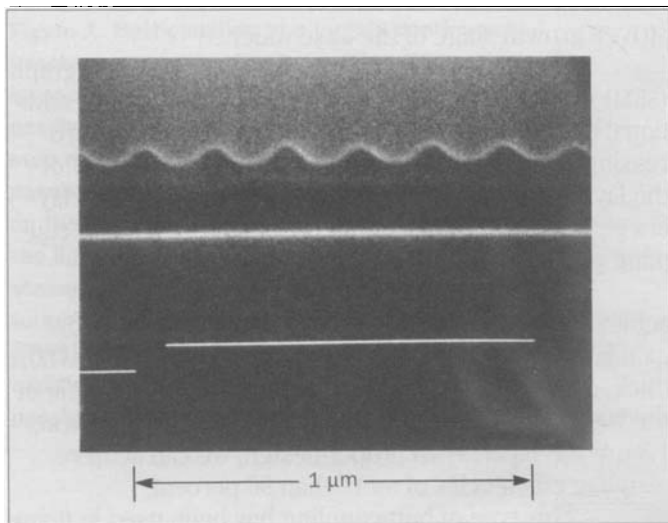


**Figure 2. SEM of a stained corrugated-waveguide grating in a 1.3- $\mu\text{m}$  DFB laser. The corrugation is visible at the interface of the higher index core material and the lower index cladding material.**

**Multisection MQW-DBR Lasers.** One simple example of a PIC that uses the techniques described earlier is the continuously tunable, multisection, MQW-DBR laser.<sup>7</sup> Here, DBR is an acronym for distributed Bragg reflector. It means that a reflection from the transparent corrugated waveguide provides one or both of the mirrors in such a laser, as we show schematically in Figure 3a. Devices of this type can justifiably be called PICs because the resonators consist of a serial coupling of three distinct guided-wave devices:

- A separate, electronically controlled gain medium
- A variable phase shifter
- A tunable, Bragg-reflection filter.

These devices have outputs of 20 to 30 mW (milliwatts), and minimum linewidths of 1 to 2 MHz (megahertz). The devices offer continuous, rapid, electronically controlled access to a 1000-GHz (gigahertz) tuning range (i.e., 80 $\text{\AA}$ ) at 1.53  $\mu\text{m}$ .

These devices have a simple operating principle. As described earlier, the corrugated waveguide provides a strong reflection only over a narrow wavelength band. The reflectivity band selects one of the longitudinal modes or standing-wave "organ-pipe" resonances of the cavity. When current is passed through the grating, the waveguide's index of refraction changes; thus, the high-

reflectivity band shifts in wavelength. Because of the band shift, longitudinal resonances of different wavelength are selected successively in the laser cavity. The phase section, if included, also operates by changing its index with current. This provides a way to alter the optical-path length of the laser cavity and continuously shift the wavelength of a particular longitudinal resonance for continuous tuning.

Devices such as this (or simpler, two-section, discretely tunable versions) may be of interest for WDM transmission systems, as discussed earlier. Such devices have also served as the basis for research demonstrations of random-access, multichannel, coherent networks with receiver sensitivities that approach the quantum limits of detection.<sup>8</sup> (We refer to this as approaching a *quantum-limited detection sensitivity*.)

**WDM Source PIC.** Figure 3b shows an extension of the tunable laser that uses a network of passive waveguides to form a WDM transmission-source PIC.<sup>9</sup> The outputs of four tunable MQW-DBR lasers are combined into a single-waveguide output port. These particular lasers are designed for independent, but simultaneous, high-speed modulation. This PIC also includes an on-chip, MQW optical-output amplifier to recover part of the losses from the power-combining operation.

One serious area of concern in PICs that use several transmitters is the potential for crosstalk between channels. This crosstalk may occur through electrical leakage on the chip or through amplifier-saturation effects. In an MQW amplifier, the latter effect is minimized because such devices have been shown to have very large saturation powers.

To investigate crosstalk in a large-signal digital environment, we modulated each laser at 2 Gb/s (gigabits per second), for an aggregate bit rate of 8 Gb/s for the combined 1.5- $\mu\text{m}$  signals. The signals, set to a 25 $\text{\AA}$  channel spacing, were successfully transmitted error-free over a 36-km (kilometer) transmission path of conventional fiber, which has low dispersion at 1.3  $\mu\text{m}$  but is quite dispersive at 1.5  $\mu\text{m}$ .

**DBR Laser, Integrated Backface Monitor.** PICs similar to the tunable DBR laser have been fabricated without the phase section. Instead, they include an additional gain section that follows the Bragg reflector and is identical to the laser gain section inside the laser resonator.

In these PICs, the second gain or active section is run with zero or reverse bias and is absorptive at the

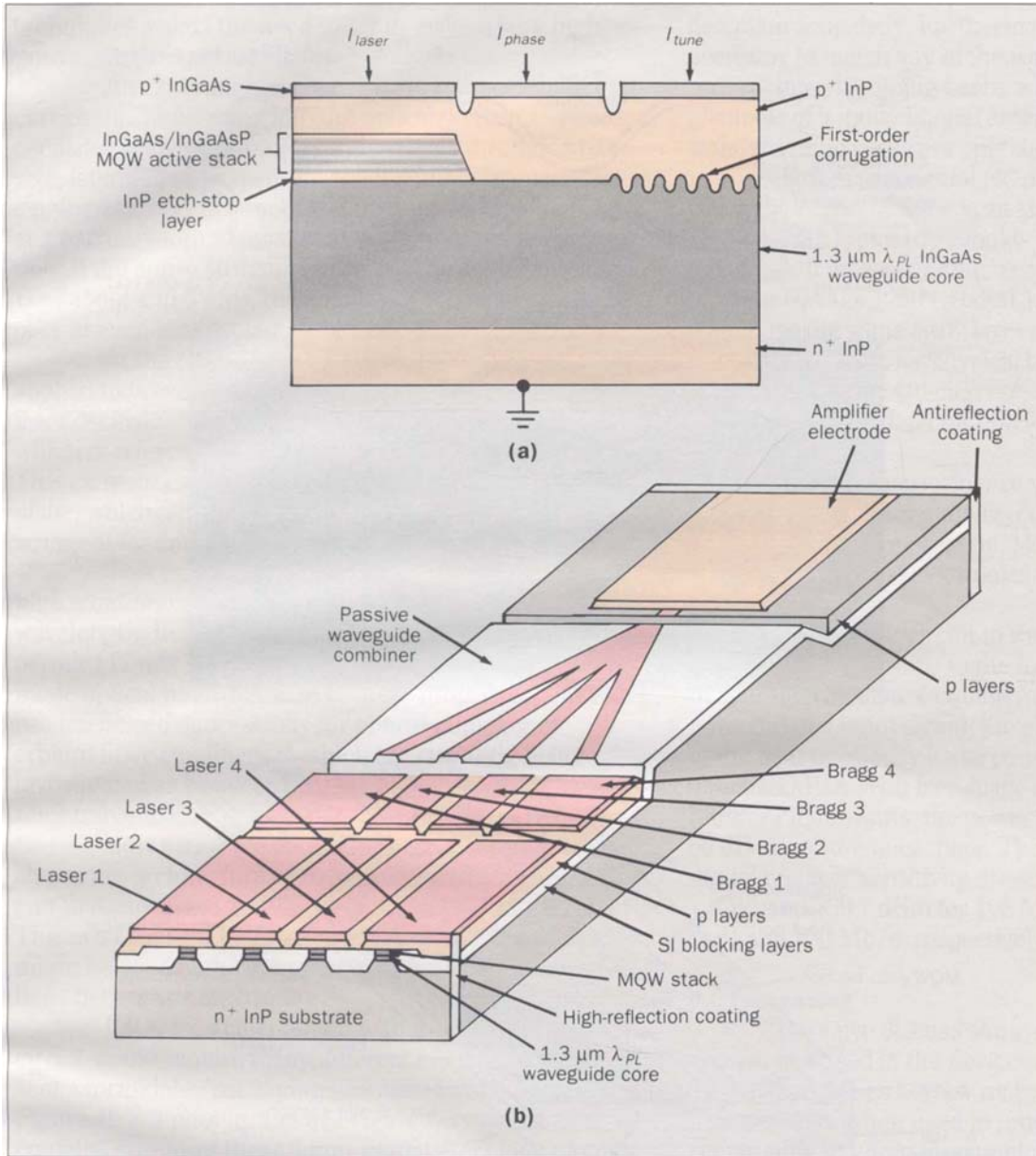


**Figure 3. Multisection MQW-DBR lasers.** (a) This continuously tunable, three-section MQW-DBR laser uses an active-to-passive transition and a corrugated-wave grating.  $I_{laser}$ ,  $I_{phase}$ , and  $I_{tune}$  identify currents applied to the respective contacts. (b) This WDM PIC has four tunable MQW-DBR lasers that combine through an MQW amplifier to a single waveguide, fiber-coupling output port.

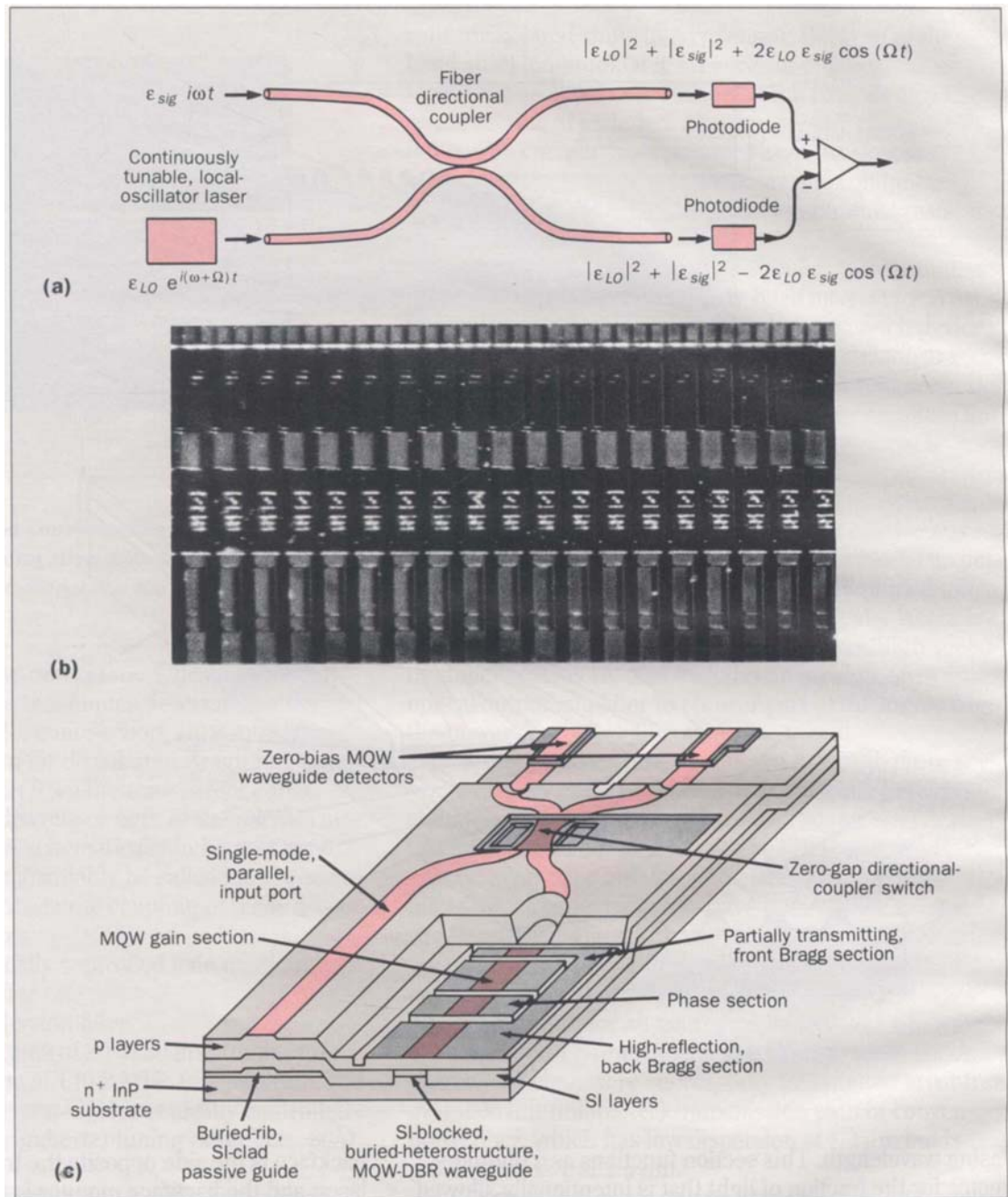
lasing wavelength. This section functions as a photodetector for the fraction of light that is intentionally allowed to leak through a short Bragg reflector. As a result, the section serves as an integrated monitor of the optical power in the laser cavity. Hence, the section could be used to replace the optics and packaging associated with providing a discrete, backface-monitor photodetector inside today's commercial laser transmitters. (The

backface is the side opposite the transmitting side of a laser, and the backface monitor is used to monitor the laser's output power.)

Such integrated devices have exhibited high detection efficiency. The combined efficiency of the laser, passive-waveguide coupling, and photodetector is still in the 30- to 40-percent range.

Other interesting applications of these integrated

**Figure 4. Heterodyne PICs. (a) Operational principle of a typical experimental fiber-optic heterodyne receiver. (b) Photograph of a cleaved, single-crystal bar that contains dozens of 3-mm long, integrated, heterodyne receiver circuits. (c) Schematic of an MQW balanced, heterodyne receiver PIC that contains a continuously tunable local oscillator (LO); a low-loss, buried-rib, parallel input port; an adjustable 3-dB coupler; and two zero-bias, MQW waveguide detectors.**



detectors use the variation in the light transmitted through the Bragg mirror as the mirror is tuned by current away from the lasing wavelength. With a feedback loop, this technique has allowed a simple external circuit to lock the Bragg mirror on the center of the laser's

longitudinal-cavity mode to guarantee stable, single-frequency operation.<sup>10</sup>

**DBR Laser, Integrated Power Amplifier.** When high power is required in radio-frequency applications, a power amplifier follows a low-power oscillator. This

techniques avoids the need to try to make a very high power, single-stage oscillator.

An experimental research PIC has been built that carries this philosophy into the optical domain.<sup>11</sup> The oscillator is an MQW-DBR laser that feeds through a passive, lateral-mode expansion section into a larger width, single-pass, optical amplifier. The laser waveguide is kept at a narrow width to provide stable lateral-mode operation. If the entire structure were as wide as the amplifier (i.e., about 4 to 5  $\mu\text{m}$ ), the stability of the beam would be poor at even modest output powers.

At the output end, an antireflection coating is applied to prevent reflected light from disturbing the laser oscillator. Also present is a waveguide element, which is referred to as an *adiabatic mode expander*.<sup>12</sup> This element expands the optical beam in the vertical plane, which permits the alignment tolerances to be less stringent for coupling to optical fibers.

This experimental PIC has produced record-high, continuous output powers of 370 mW at a 1.48- $\mu\text{m}$  wavelength. In addition, the beam was stable enough to permit 117 mW of power to be coupled into a single-mode optical fiber. Because of these properties, this PIC has been used successfully for optical pumping of erbium fiber amplifiers,<sup>13</sup> which are currently being investigated as replacements for digital repeaters in long fiber-transmission spans.

**MQW Balanced Heterodyne Receiver PIC.** Figure 4a shows the architecture of another relatively complex circuit that was demonstrated recently in PIC form at AT&T. This is a balanced heterodyne receiver of the sort that might be used in the coherent lightwave communications networks of the future.

If it were implemented with discrete devices, this circuit would require many different elements and present a formidable packaging problem. For comparison, Figure 4b is a photograph of a cleaved-crystal bar that contains dozens of these 3-mm (millimeter) long circuits.

A detailed schematic of the balanced heterodyne receiver PIC appears in Figure 4c. Heterodyne reception uses a high-power, tunable *local oscillator* (LO) laser that is set to a frequency nearly equal to that of the weak incoming signal. The beams are then combined into photodetectors. Because it detects the current at the beat note or difference frequency (which is much larger than the current that arises from just the weaker incoming signal), the device can approach a quantum-limited

detection sensitivity. Furthermore, if we tune the local oscillator to match any of the wavelengths that might be present in an incoming beam, we can select individual channels of a multichannel *broadcast*. This is exactly how standard radio receivers operate.

This experimental PIC performs quite successfully.<sup>14</sup> The LO laser is an MQW-DBR (as discussed earlier), with typical thresholds of 20 to 35 mA (milliamperes). It offers continuous access to a tuning range of about 60  $\text{\AA}$  (i.e., 750 GHz) at 1.53  $\mu\text{m}$ . The detectors, which use the same MQW layers for absorption as the laser does for gain, have typical bandwidths of 1 to 2 GHz into 50-ohm loads. On-chip optical losses and departures from 100-percent detector efficiency totaled only -4.3 dB (decibels).

The PIC's performance was evaluated while it received a frequency-shift-keyed, digital format signal from a remote, three-section, MQW-DBR transmitter. Only 50-ohm commercial electronics were connected directly to the PIC.

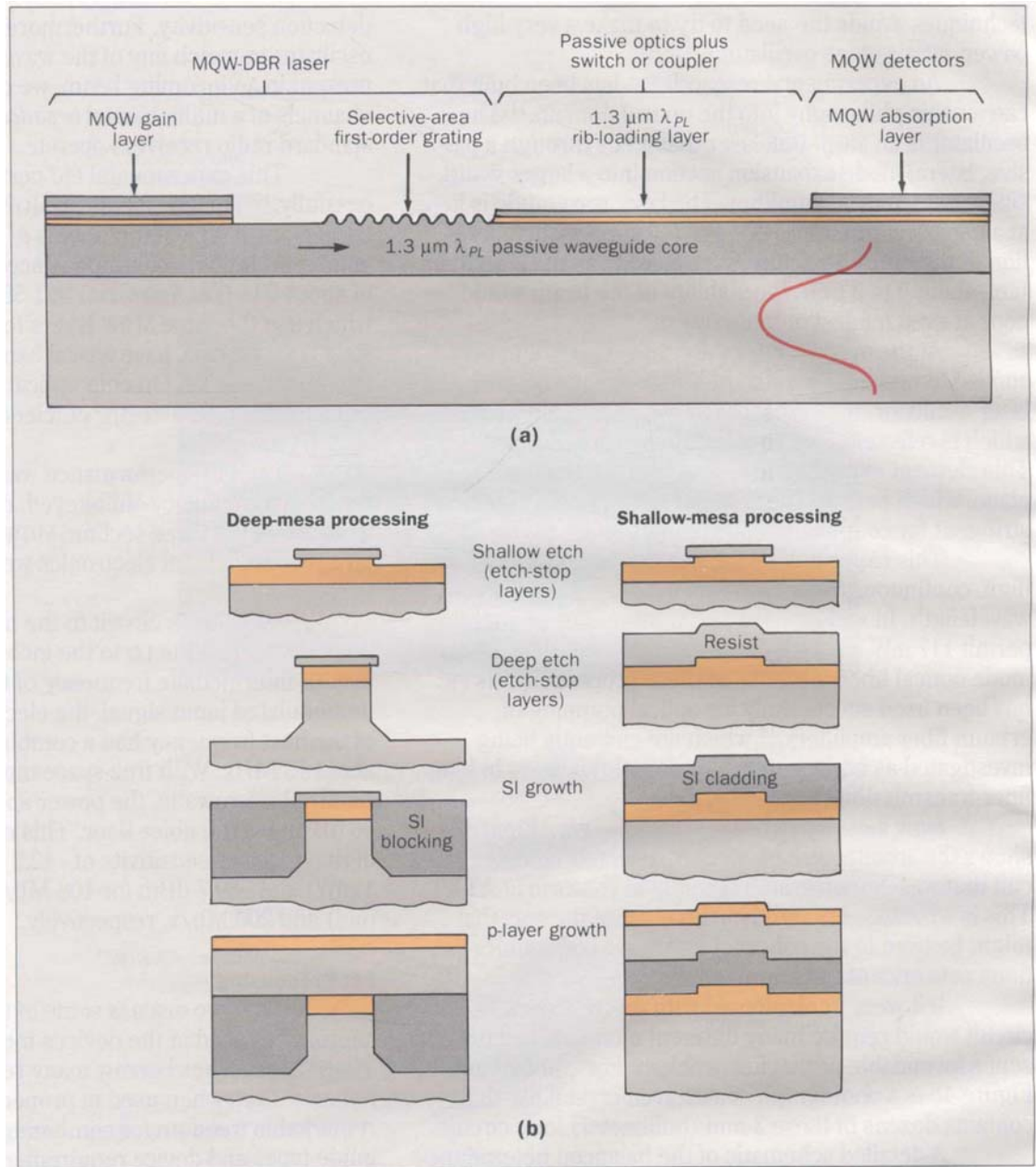
A feedback circuit to the tunable LO laser automatically locked the LO to the incoming signal at a typical beat or intermediate frequency of 600 MHz. With an unmodulated input signal, the electrical power spectrum of the beat frequency had a combined -3 dB linewidth of about 13 MHz. With free-space input beams of several hundred microwatts, the power spectrum rose about 60 dB above the noise floor. This resulted in a measured, digital-receiver sensitivity of -42.3 dBm (decibels below 1 mW) and -39.7 dBm for 108 Mb/s (megabits per second) and 200 Mb/s, respectively.

### PIC Processing

Here, we discuss some of the fabrication approaches used in the devices mentioned previously. These approaches borrow many refined processing techniques<sup>15</sup> that, when used in proper sequence, offer remarkable freedom for combining the various waveguide types and device requirements without undue growth complexity. We will focus on a variant of PPro-2, a fabrication process.<sup>16</sup> This variant illustrates how the relatively complex PICs we have described can be fabricated without additional growth steps beyond those required to process commercial lasers.

In PPro-2, one can separate the processing and growth conceptually into two stages: longitudinal processing and lateral processing.

**Figure 5. PIC processing stages. (a) Longitudinal processing sequence for the waveguide stack. (b) Simultaneous, self-aligned lateral processing of the active, buried-heterostructure region and passive, low-loss, buried-rib region. Deep-mesa processing is used for buried heterostructures (e.g., lasers and detectors), while shallow mesas are for buried ribs (e.g., passive waveguides and couplers).**



The first stage consists of growing the base wafer up to and including all passive core and active layers of the waveguide. In a broad-area processing sequence, the wafer then undergoes *longitudinal processing* as illustrated in Figure 5a. Here, the processing consists of:

1. Removal of the active MQW stack, except in the gain and detector portions of the PIC. A wet-chemical etch

is used that is material selective, and the depth is controlled by the etch-stop layer.

2. Removal of a buried rib-loading layer where it is not needed. This step also uses selective etching.
3. Selective placement of first-order gratings, where desired. This step uses conventional holographic exposure and wet etching.

The longitudinal-processing stage thus creates a longitudinally continuous, slab waveguide that has a vertical structure suited to each device type. The only mismatch results from the perturbation induced by the removal of thin layers, as discussed earlier.

After the broad-area longitudinal processing, the stripe is defined in a *lateral-processing* sequence. The sequence allows the same growths to perform different functions in different portions of the PIC; i.e.,

- The oxide-stripe waveguide etch mask is patterned.
- Two paths are then followed. One path produces buried-heterostructure waveguide devices (i.e., lasers, detectors, modulators, etc.). The other results in buried-rib devices (i.e., passive waveguides, directional couplers, etc.).

Figure 5b illustrates this process. (Figure 5a showed the guiding layers separately. For simplicity, we show the entire sequence of guiding layers as one layer here.)

Lateral processing consists of these steps:

1. A shallow etch defines the rib everywhere. The depth of the etch is controlled by an etch-stop layer in regions where the rib waveguide is the intended final structure. The oxide is then removed in the rib-waveguide regions and replaced with resist.
2. Next, a deep etch is carried out in the unprotected regions. Here, too, the depth is controlled by etch-stop layers.
3. After the deep etch, a regrowth sequence produces a semi-insulating InP (SI-InP) blocking layer. This growth provides low-loss upper cladding in passive regions, but forms lateral blocking in the deep-mesa active devices. If current or field access is desired in any rib waveguides that were overgrown with SI-InP, the SI-InP can be removed locally.
4. After final removal of the oxide on the deep-mesa devices, one grows the p-type, upper-cladding layers.

This combination of longitudinal and lateral processing is powerful. With only three growth steps, it can produce vertically and laterally self-aligned waveguides of various types, each suited to a particular device.

Another advantage of the SI-InP, upper-clad, buried-rib waveguides is the potential for high electrical isolation between different portions of the PIC. Because we can selectively remove the upper p-layers over the passive, buried-rib waveguide regions, we can readily achieve complete (i.e., megohm-level) isolation between devices.

## Conclusion

We have provided examples of experimental PICs from several different application areas. These examples were selected to illustrate current design concepts and current approaches to PIC growth and fabrication.

The advances seen in this field in recent years have stemmed largely from basic improvements in crystal-growth technology. However, we have only begun to explore the freedom that quantum-well growth capabilities, large-area uniformity, and complex vertical-layer structures will offer to device design and fabrication engineering. The coming years should provide exciting opportunities for novel PIC designs, as well as hope for early commercial realizations as the field of optical communications continues to mature.

## Acknowledgment

We would like to thank our many colleagues and collaborators at AT&T Bell Laboratories. Without their contributions, many of the illustrative examples presented here would not have been possible.

## References

1. S. E. Miller, "Integrated Optics: An Introduction," *Bell System Technical Journal*, Vol. 48, 1969, pp. 2059-2069.
2. H. Kogelnik, "Integrated Optics, OEIC's or PIC's?," *International Trends in Optics*, J. W. Goodman (ed.), Academic Press, Orlando, Florida, 1991, pp. 1-12.
3. T. L. Koch and U. Koren, "Semiconductor Photonic Integrated Circuits," *IEEE Journal of Quantum Electronics*, Vol. QE-27, 1991, pp. 641-653.
4. P. K. Bohn, M. J. Kania, J. M. Nemchik, and R. C. Purkey, "Fiber in the Loop," *AT&T Technical Journal*, Vol. 71, No. 1, January/February 1992, pp. 31-45.
5. A. Y. Cho and A. M. Glass, "Photonic Materials and Processing," *AT&T Technical Journal*, Vol. 69, No. 6, November/December 1990, pp. 77-91.
6. M. Suzuki, Y. Noda, H. Tanaka, S. Akiba, Y. Kushiro, and H. Isshiki, "Monolithic Integration of InGaAsP/InP Distributed Feedback Laser and Electroabsorption Modulator by Vapor Phase Epitaxy," *IEEE Journal of Lightwave Technology*, Vol. LT-5, 1987, pp. 1277-1285.
7. T. L. Koch, U. Koren, R. P. Gnall, C. A. Burrus, and B. I. Miller, "Continuously Tunable 1.5  $\mu\text{m}$  Multiple-Quantum-Well InGaAs/InGaAsP Distributed-Bragg-Reflector Lasers," *Electronics Letters*, Vol. 24, 1988, pp. 1431-1432.
8. B. Glance, T. L. Koch, O. Scaramucci, K. C. Reichmann, L. D. Tzeng, U. Koren, and C. A. Burrus, "Densely Spaced FDM Optical Coherent System with Near Quantum-Limited Sensitivity and Computer-Controlled Random Access Channel Selection," *Electronics Letters*, Vol. 25, 1989, pp. 883-885.
9. A. H. Gnauck, U. Koren, T. L. Koch, F. S. Choa, C. A. Burrus, G. Eisenstein, and G. Raybon, "Four-Channel WDM Transmission

- Experiment Using a Photonic-Integrated-Circuit Transmitter," *Technical Digest, OFC '90, Optical Fiber Communications Conference, Post Deadline Papers*, San Francisco, California, January 22 to 26, 1990, Optical Society of America, Washington, D.C., 1990, pp. PD26-1-PD26-4.
10. S. L. Woodward, T. L. Koch, and U. Koren, "Control Loop Which Insures High Side-Mode Suppression in Tunable DBR Lasers," *LEOS '91, Conference Digest, IEEE Lasers and Electro-Optics Society Annual Meeting*, San Jose, California, November 4 to 7, 1991, Institute of Electrical and Electronics Engineers, New York, 1991, p. 82.
  11. U. Koren, R. M. Jopson, B. I. Miller, M. Chien, M. G. Young, C. A. Burrus, C. R. Giles, G. Raybon, J. D. Evankow, B. Tell, and K. Brown-Goebeler, "High Power Laser-Amplifier Photonic Integrated Circuit for 1.48  $\mu\text{m}$  Operation," *Technical Digest, OFC '91, Optical Fiber Communications Conference, Post Deadline Papers*, San Diego, California, February 18 to 22, 1991, Optical Society of America, Washington, D.C., 1991, paper PD10, pp. 49-52.
  12. T. L. Koch, U. Koren, G. Eisenstein, M. G. Young, M. Oron, C. R. Giles, and B. I. Miller, "Tapered Waveguide InGaAs/InGaAsP Multiple Quantum Well Lasers," *IEEE Photonics Technology Letters*, Vol. 2, 1990, pp. 88-90.
  13. J. L. Zyskind, C. R. Giles, J. R. Simpson, and D. J. DiGiovanni, "Erbium-Doped Fiber Amplifiers and the Next Generation of Light-wave Systems," *AT&T Technical Journal*, Vol. 71, No. 1, January/February 1991, pp. 53-62.
  14. T. L. Koch, F. S. Choa, U. Koren, R. P. Gnall, F. Hernandez-Gil, C. A. Burrus, M. G. Young, M. Oron, and B. I. Miller, "Balanced Operation of an InGaAs/InGaAsP Multiple-Quantum-Well Integrated Heterodyne Receiver," *IEEE Photonics Technology Letters*, Vol. 2, 1990, pp. 577-580.
  15. W. C. Dautremont-Smith, R. J. McCoy, R. H. Burton, and A. G. Baca, "Fabrication Technologies for III-V Compound Semiconductor Photonic and Electronic Devices," *AT&T Technical Journal*, Vol. 68, No. 1, January/February 1989, pp. 64-82.
  16. U. Koren, T. L. Koch, B. I. Miller, and A. Shahar, "Processes for Large Scale Photonic Integrated Circuits," *Technical Digest, Integrated and Guided Wave Optics Conference*, Houston, Texas, February 6 to 8, 1989, Optical Society of America, Washington, D.C., 1989, paper MDD2, pp. 68-71.

(Manuscript received August 1, 1991)

**Thomas L. Koch** is head of the Optoelectronics Research Department with AT&T Bell Laboratories in Holmdel, New Jersey. He manages research on optoelectronic devices, circuits, and subsystems used in optical-fiber communications. Mr. Koch joined the company in 1982 and holds an A.B. degree in physics from Princeton University (New Jersey) and a Ph.D. in applied physics from the California Institute of Technology (Pasadena).

**Uziel Koren** is a supervisor in the Optoelectronics Research Department at AT&T Bell Laboratories in Holmdel, New Jersey. He is responsible for research on lasers and photonic devices for telecommunications. Mr. Koren joined the company in 1983 and has a B.Sc., an M.Sc., and a Ph.D. in physics from Weizmann Institute of Science, Rehovot, Israel.